The Journal of Immunology

RESEARCH ARTICLE | SEPTEMBER 15 2004

A Novel Mutation in IFN-γ Receptor 2 with Dominant Negative Activity: Biological Consequences of Homozygous and Heterozygous States[1] FREE

Sergio D. Rosenzweig; ... et. al

J Immunol (2004) 173 (6): 4000–4008.
https://doi.org/10.4049/jimmunol.173.6.4000

A Novel Mutation in IFN-γ Receptor 2 with Dominant Negative Activity: Biological Consequences of Homozygous and Heterozygous States[1]

Sergio D. Rosenzweig,[2]* Susan E. Dorman,* Gulbu Uzel,* Stephen Shaw,‡ Amy Scurlock,‡ Margaret R. Brown,§ Rebecca H. Buckley,‡ and Steven M. Holland[3†]

We identified two siblings homozygous for a single base pair deletion in the IFN-γR2 transmembrane domain (791delG) who presented with multifocal *Mycobacterium abscessus* osteomyelitis (patient 1) and disseminated CMV and *Mycobacterium avium* complex infection (patient 2), respectively. Although the patients showed no IFN-γR activity, their healthy heterozygous parents showed only partial IFN-γR activity. An HLA-identical bone marrow transplant from the mother led patient 1 to complete hemopoietic reconstitution, but only partial IFN-γR function. We cloned and expressed fluorescent fusion proteins of the wild-type IFN-γR2, an IFN-γR2 mutant previously described to produce a complete autosomal recessive deficiency (278del2), and of 791delG to determine whether the intermediate phenotype in the 791delG heterozygous state was caused by haploinsufficiency or a dominant negative effect. When cotransfected together with the wild-type vector into IFN-γR2-deficient fibroblasts, the fusion protein with 791delG inhibited IFN-γR function by 48.7 ± 5%, whereas fusion proteins with 278del2 had no inhibitory effect. Confocal microscopy of 791delG fusion proteins showed aberrant diffuse intracellular accumulation without plasma membrane localization. The fusion protein created by 791delG did not complete Golgi processing, and was neither expressed on the plasma membrane, nor shed extracellularly. The mutant construct 791delG exerts dominant negative effects on IFN-γ signaling without cell surface display, suggesting that it is acting on pathways other than those involved in cell surface recognition of ligand. ***The Journal of Immunology*****, 2004, 173: 4000–4008.**

The functional IFN-γR complex is formed by two IFN-γR1 and two IFN-γR2 molecules brought together by the binding of IFN-γ (reviewed in Ref. 1). Both receptors belong to the class 2 cytokine receptor family, which are molecules devoid of intrinsic phosphatase or kinase activity. IFN-γR1 maps to chromosome 6 and consists of seven exons; exon 7 harbors a Jak1 binding site and a STAT1 docking site. IFN-γR2 maps to chromosome 21q22.1 and also consists of seven exons; exon 7 contains a Jak2 binding site. Although IFN-γR1 is constitutively expressed on all nucleated cells, IFN-γR2 membrane display is quite limited and tightly regulated. Intracellular levels of IFN-γR2 are significantly higher than those displayed on the cell surface. Information regarding IFN-γR2 recycling and the factors regulating IFN-γR2 recycling and fate are incompletely understood (1–8). One of the major limitations in this regard has been the paucity of histochemical and biochemical reagents for detection of IFN-γR2.

The majority of defects leading to impaired IFN-γ signaling have been detected in IFN-γR1, due to both recessively and dominantly inherited mutations. In general, recessive mutations map to the extracellular domain of IFN-γR1, whereas dominant mutations map to the intracellular domain (9–16).

Two different mutations have been reported in IFN-γR2, both recessively inherited. One caused recessive complete IFN-γR2 deficiency (278delAG) (17) and the other caused a recessive partial IFN-γR2 deficiency (Cys340Thr) (18); both map to the extracellular domain. We report an IFN-γR2 mutation that was detected in the homozygous state as causing complete IFN-γR2 deficiency. However, the recognition of a heterozygous in vitro phenotype in the parents of the affected children and in one child after complete hemopoietic reconstitution from the heterozygous mother, led us to examine in more detail the cellular function of this mutation. Because commercially available Abs for IFN-γR2 detection are inadequately sensitive for the tracking the cellular distribution of native proteins, we created a series of fluorescent fusion proteins.

Materials and Methods

Patients

Patient 1 was a firstborn girl to Qatari first cousins. Pregnancy and perinatal course were uneventful; birth weight was 3.19 kg. At age 2 days, bacillus Calmette-Guérin (BCG)[4] vaccine was administered in the left arm. At age 3 wk the patient developed signs consistent with disseminated BCG infection: fever, generalized rash, left axillary lymphadenopathy and hepatosplenomegaly. Liver biopsy showed microgranulomata and acid-fast organisms. Antituberculous therapy resulted in apparent cure. At age 15 mo,

*Laboratory of Host Defenses, and †Laboratory of Clinical Infectious Diseases, National Institute of Allergy and Infectious Diseases, and ‡Clinical Immunology Laboratory, Warren Grant Magnuson Clinical Center, National Institutes of Health, Bethesda, MD 20892; and §Departments of Pediatrics and Immunology, Duke University Medical Center, Durham, NC 27710

Received for publication July 30, 2003. Accepted for publication June 30, 2004.

The costs of publication of this article were defrayed in part by the payment of page charges. This article must therefore be hereby marked *advertisement* in accordance with 18 U.S.C. Section 1734 solely to indicate this fact.

[1] This work was supported by the National Institutes of Health Fogarty International Center, and by the Fogarty International Research Collaboration Award Grant R01 TW006644 (to S.D.R.).

[2] Current address: Servicio de Inmunologia, Hospital Nacional de Pediatria "J. P. Garrahan," Combate de los Pozos 1881, Ciudad de Buenos Aires 1245, Argentina

[3] Address correspondence and reprint requests to Dr. Steven M. Holland, MD, Laboratory of Clinical Infectious Diseases, National Institute of Allergy and Infectious Diseases, National Institutes of Health, Building 10, Room 11N103, 10 Center Drive, Mail Stop Code 1886, Bethesda, MD 20892. E-mail address: smh@nih.gov

[4] Abbreviations used in this paper: BCG, bacillus Calmette-Guérin; MP, mature protein; SP, signal peptide; eGFP, enhanced GFP; RFP, red fluorescent protein; EndoH, endoglycosidase H.

0022-1767/04/$02.00

rash, lymphadenopathy, and hepatomegaly recurred. Right leg tenderness prompted a bone scan, which showed osteomyelitis of the right femur, right tibia, and mandible. *Mycobacterium abscessus* was isolated from blood and a lymph node biopsy. Multidrug therapy and s.c. IFN-γ were started. Culture of the urine was positive for CMV. HIV testing was negative. The white blood cell count was 34,800/μl, and the erythrocyte sedimentation rate was 119 mm/h. Serum Igs were normal to slightly elevated.

Evaluation at Duke University Medical Center (Durham, NC) showed $CD3^+$ 5613/μl (58%), $CD4^+$ 2836/μl (29%), and a CD4 to CD8 ratio of 1.0; proliferations to PHA, purified protein derivative, and tetanus toxoid were normal, but to concanavalin A, pokeweed mitogen, and *Candida* were diminished (Table I). Surface display of the IFN-γR1 on monocytes was normal. Given that this was the child's second disseminated mycobacterial infection, the lack of complete control of *M. abscessus* infection despite 3 mo of antibiotics and s.c. IFN-γ treatment and the high probability of future serious infections, bone marrow transplantation was considered. The patient and her mother were found to be HLA identical. After busulfan and cyclophosphamide conditioning, the patient was transplanted with 2.8×10^8/kg unfractionated maternal bone marrow nucleated cells. Adjunctive IFN-γ was stopped just before conditioning; clarithromycin and amikacin were continued after bone marrow transfusion. Patient 1 developed grade III acute graft-versus-host disease of the skin on day 9 and graft-versus-host disease of the gut on day 50, successfully treated with tacrolimus, corticosteroids, and anti-CD25 Ab. Lymphadenopathy resolved with bone marrow engraftment and blood cultures remained negative for mycobacteria. By day +26, bone scans showed significant healing of all involved sites. One month after transplantation all cell lineages were recovered, and genetic analysis of PBMC based on restriction fragment length polymorphisms demonstrated full donor marrow engraftment. Functional analysis of patient PBMC done 8 mo after transplantation showed partial reconstitution of IFN-γR function as evaluated by TNF-α response to IFN-γ stimulation. Two months later while in otherwise good health, the patient developed fulminant catheter-associated *Serratia marcescens* septicemia and died. An autopsy was not permitted.

Patient 2 is the brother of patient 1 and the only sibling. Pregnancy was complicated by maternal flu-like illness at 3 mo gestation. Newborn screening showed glucose-6-phosphate dehydrogenase deficiency and thalassemia major. BCG vaccine was not administered due to the sister's history. He developed a viral exanthem on day 20. At age 2 mo he developed oral candidiasis and hepatosplenomegaly with an elevated CMV IgM Ab titer and positive urine cultures for CMV. Blood CMV antigenemia was absent. Mycobacterial cultures from blood and urine were negative. He had normal or elevated serum Igs and diphtheria and tetanus titers, normal lymphocyte subpopulations, and normal proliferative responses to mitogens and Ags (Table I). Urine cultures continued to grow CMV despite 2 mo of ganciclovir. Patient 2 received oral azithromycin prophylaxis and valganciclovir therapy. He was admitted to a Qatari hospital at age 4 mo with fever, anemia, hepatosplenomegaly, rash, and coagulopathy. Acid-fast bacilli were identified microscopically from a blood specimen, but did not grow. Focal lesions in the spleen and hepatosplenomegaly were detected. The patient was transferred to Duke University Medical Center for possible bone marrow transplantation, where a blood culture was positive for *M. avium*, and CMV DNA was detected in his blood. He was subsequently found to have numerous splenic and cerebral mycobacterial abscesses. At resection the spleen showed necrotic granulomata, and grew *M. avium*. He was treated aggressively for mycobacteria and CMV and received an unfractionated bone marrow transplant from his HLA-identical father.

Molecular analysis of IFN-γR2 gene (IFNGR2)

For patient 1, the seven exons of IFNGR1 and IFNGR2 were examined by sequencing of genomic DNA; for parents and patient 2, IFNGR2 exon 6 was sequenced from genomic DNA using primers 5′-GTGCGTAGAA GATCATTCTG-3′ (forward), and 5′-GATGTGTGCACACGTACCTC-3′ (reverse). The PCR products were purified and sequenced with the Sequenase Cyclist TaqDNA Sequencing kit (Stratagene, La Jolla, CA) according to the manufacturer's instructions.

Total RNA was extracted (RNA STAT-60; Tel-Test, Friendswood, TX) and cDNA converted (ThermoScript RT-PCR system; Invitrogen Life Technologies, Carlsbad, CA) from EBV-transformed B cell lines from patient 1, parents, and a normal control. The cDNAs were PCR-amplified using IFNGR2 exonic primers spanning the mutation site: forward primer (exon 5) 5′-CCAGGCACAACTGCTTTGGAAC-3′; reverse primer (exon 6, downstream to mutation 791delG) 5′-CAGGACCAGGAAGAAA CAGGC-3′. The expected amplimer length for cDNA was 214 bp. The PCR products were purified (Geneclean II; Bio101, Carlsbad, CA) and digested with AlwN I (New England Biolabs, Beverly, MA) following the manufacturer's recommendations. Mutation 791delG creates a novel AlwN I restriction site.

In vitro cytokine production and response

PBMC were prepared and stimulated with *Escherichia coli*-derived LPS (Sigma-Aldrich, St. Louis, MO), or LPS plus IFN-γ (Genentech, South San Francisco, CA) as described (17). Supernatants were examined for TNF-α concentration in duplicate by ELISA (R&D Systems, Minneapolis, MN).

FACS analysis

Flow cytometric analysis of IFN-γ-induced phosphorylated STAT1 was performed as described (19).

Transiently transfected HEK 293 cells (1×10^6) were incubated with 1 μg of mouse anti-GFP mAb (JL-8; Clontech Laboratories, Palo Alto, CA) for 30 min at 4°C. Cells were washed and incubated with a rat anti-mouse PerCP-labeled secondary Ab. Twenty-five thousand events were acquired in a FACScan flow cytometer and analyzed using CellQuest (BD Biosciences, San Jose, CA).

Constructs

The cDNA sequences for the IFNGR2 mature protein (MP) and signal peptide (SP) were separately cloned with enhanced GFP (eGFP) into the p-eGFP-C1 vector (Clontech Laboratories), resulting in the construct: 5′-SP/GFP/MP-3′ expressing a GFP-IFN-γR2 fusion protein. American Type

Table I. *Immunologic data in a model of IFNγR2 mutation detected in homozygous and heterozygous states*

	Patient 1	Patient 2	Normal Range
Serum Igs (mg/dl)			
IgG	1153	1270	356–952
IgA	118	15	12–73
IgM	179	189	43–174
IgE IU/ml	19	3	0–150
Lymphocyte subpopulations (per cm^2)			
CD3	5613	4194	1014–5784
CD4	2836	1767	567–3725
CD8	2816	2411	390–2673
CD16	146	1792	87–1189
CD20	2270	1742	121–1072
Lymphocyte responses (cpm)			
Medium control	1247	633	693 ± 825
PHA	217,112	229,009	222,330 ± 50,643
Con A	125,170	163,114	208,534 ± 52,592
Pokeweed mitogen	47,227	76,635	135,520 ± 35,077
Tetanus toxoid	76,267	168,110	42,527 ± 5900

Culture Collection (ATCC) IFNGR2 was used as template (ATCC no. 79923; *Eco*RI-*Eco*RI cloned in pBluescript vector). We engineered an *Eco*RI site 3 bp upstream of the first codon of the IFNGR2 MP sequence, forward primer, 5′-CGCCAGACCCGAATTCCCAGCTGCTGCCCGCT CCTCAGCAC-3′, first codon of the IFNGR2 MP sequence underlined; reverse primer, downstream of the ATCC IFNGR2 distal *Eco*RI cloning site, 5′-GAGCGCGCGTAATACGACTCACTATAGGG-3′). The resulting PCR product and the p-eGFP-C1 vector were *Eco*RI digested (Invitrogen Life Technologies), purified (Geneclean II, Bio101) and ligated with the TaKaRa ligation kit following the producer's recommendations (Takara Shuzo, Otsu, Japan). DH5-α competent bacteria were transformed and grown on Luria-Bertani-kanamycin plates. Colonies were selected and checked for insertion and orientation by PCR. Using the same IFNGR2 cDNA ATCC clone as template, *Eco*47 III sites were introduced by PCR on either side of the IFNGR2 SP cDNA sequence forward primer 5′-CGC-CGCCGAGCGCTCCGGGGCCATG-3′ underlined, first codon of the IFNGR2 SP cDNA sequence; reverse primer 5′-GTACAGGCGTAGCGCT GGCTGCTGAGG-3′; *Eco*47 III site created nine amino acids into the IFNGR2 MP cDNA sequence). The resulting PCR product and the GFP/IFNGR2 MP construct were *Eco*47 III digested (Invitrogen Life Tecgnologies) and the products ligated to create the construct SP/GFP/IFNGR2. The complete inserts and the boundaries were sequenced and confirmed to be appropriate.

The GFP sequence was removed from construct SP/GFP/IFNGR2 and replaced by the red fluorescent protein (RFP) sequence from vector pDsRed2/C1 (Clontech Laboratories). Briefly, both vectors were sequentially digested with restriction enzymes *Pin*A I and *Bgl*II (Invitrogen Life Technologies). The two enzymes recognize unique restriction sites upstream (*Pin*AI) and downstream (*Bgl*II) of the GFPs and the RFPs. Restriction products were gel purified (QIAquick; Qiagen, Valencia, CA) and the RFP sequence was ligated to the SP/-/IFNGR2 sequence (Takara Shuzo) producing the construct SP/RFP/IFNGR2. The sequence of the complete insert and the boundaries were confirmed to be appropriate.

Mutagenesis

The mutations 791delG and 278delAG were separately introduced into the SP/GFP/IFNGR2 construct by site-directed mutagenesis following the manufacturer's protocol (QuickChange Site Directed Mutagenesis kit; Stratagene), leading to constructs SP/GFP/791delG and SP/GFP/278del2, respectively. Mutations were verified by sequencing.

Cell lines and transfections

HEK 293 (ATCC, CRL-1573) cells were grown in DMEM with 10% FCS, 2 mM L-glutamine, and antibiotics (penicillin and streptomycin; Invitrogen Life Technologies). Cells were split every 3–4 days. SV-40-transformed fibroblasts from an IFN-γR2-deficient patient (17) were grown in Eagle's MEM with 10% FCS, 2 mM L-glutamine, 1 mM sodium pyruvate, and penicillin and streptomycin. Cells were seeded in six-well plates for 24 h. before transfection ($1–2 \times 10^5$ cells/well) and transfected over 8 h in OptiMEM (Invitrogen Life Technologies) with 5 μl of Lipofectin (Invitrogen Life Technologies) and 1–2 μg of DNA following the lipofectin-adherent cell transient transfection protocol. HEK 293 were transfected with 1 μg of DNA; IFN-γR2-deficient fibroblasts were transfected with 2 μg of DNA. In wild-type-only or mutant-only experiments, 1 μg of the relevant vector was cotransfected with 1 μg of an irrelevant vector (p-eGFP-C1) to keep total DNA content of the transfection constant. In wild-type/mutant combination experiments, 1 μg of wild-type vector was cotransfected with 1 μg of the mutant vector. After transfection, cells were grown for 48 or 72 h before evaluation. Where indicated, cells were stimulated with IFN-γ (Actimmune; Intermune, Brisbane, CA), 1000 U/ml for 15 min before harvest. Transfection efficiency, based on microscopic evaluation of GFP expression, varied between 15% and 25% for all constructs in individual vector experiments. No significant differences in transfection efficiency were found when either β-Gal and pRL-Renilla were used as normalizing agents (data not shown). For all experiments two different preparations of each construct were used and no differences were found between them.

Binding assays

Recombinant human IFN-γ (PeproTech, Rocky Hill, NJ) was labeled with Cy5 (Amersham Biosciences, Piscataway, NJ) following the manufacturer's instructions with some alterations. Briefly, the IFN-γ was diluted in PBS pH 7.4, the pH was adjusted to 9.3 with 1 M sodium carbonate, and aliquoted into three equal fractions. Lyophilized Cy5 dye was reconstituted in PBS (pH 7.4) and the appropriate amounts were added to separate fractions of the IFN-γ to deliver 0.5×, 1×, and 2× normal dye-protein labeling ratios. The reaction was incubated at room temperature for 30 min and the unconjugated dye was separated from the Cy5-IFN-γ conjugates by gel filtration. The resulting product 0.5× Cy5-IFN-γ was used to assess the ligand binding capacity of the wild-type and 791delG mutant IFN-γR2 constructs. HEK 293 cells were transiently transfected with wild-type SP/GFP/IFNGR2 and SP/GFP/791delG vectors. Cells were harvested 48 h after transfections, washed and exposed to 0.5× Cy5-IFN-γ (0.5 μg/10^6 cells) during 15 min at 4°C. Cy5 geometric mean channel was analyzed by flow cytometry in GFP-positive cells. To verify that this labeled IFN-γ was able to bind the authentic receptor, we performed flow cytometry based competition experiments with unlabeled IFN-γ as described elsewhere (20). Briefly, untransfected HEK 293 cells were incubated with 0.5× Cy5-IFN-γ (0.02 μg/10^6 cells) for 15 min at 4°C. The 0.5× Cy5-IFN-γ was competed off with increasing amounts of unlabeled IFN-γ (0.002, 0.02, 0.5, 2.5, and 10 μg/10^6 cells), and the bound Cy5 geometric mean channel determined for each concentration (data not shown).

Immunoblotting

Total cell lysates from transfected cells were prepared 48 or 72 h after transfection. Samples were resolved on 10% Bis-Tris precast gels (Novex; Invitrogen Life Technologies) and transferred to 0.2-μm pore polyvinylidene difluoride membranes (Invitrogen Life Technologies). Membranes were preblocked overnight at 4°C in a 5% blocking grade nonfat dry milk solution (Bio-Rad, Hercules, CA), probed for 1 h with the primary Ab, washed three times, and then reprobed for 30 min with HRP-conjugated secondary Ab. Blots were developed with the ECL Plus kit (Amersham Pharmacia Biotech, Little Chalfont, U.K.) according to the manufacturer's instructions. As indicated, blots were stripped for 30 min at 50°C in 50 ml of a solution (10 mM 2-ME plus 2% SDS plus 62.5 mM Tris) and reprobed.

Supernatants from p-eGFP-C1, SP/GFP/IFNGR2 and SP/GFP/791delG, HEK 293 transfected cells were collected and concentrated (Centricon; Millipore, Bedford, MA) following the manufacturer's protocol. Samples were resolved in 10% Bis-Tris precast gels (Novex).

Total cell lysates from SP/GFP/IFNGR2 and SP/GFP/791delG transiently transfected HEK 293 cells were digested with endoglycosidase H (EndoH; (New England Biolabs) following the producer's protocol. Samples were resolved in 10% Bis-Tris precast gels.

Primary Abs

Polyclonal rabbit anti-human p-STAT1 (Tyr 701) Ab (Cell Signaling, Beverly, MA) was used at 1/1000 dilution. Monoclonal mouse anti-human STAT1 Ab (BD Transduction Laboratories, Lexington, KY) was used at 1/5000 dilution. Monoclonal mouse anti-GFP Ab (Living Colors; BD Biosciences) was used at 1/1000 dilution. Polyclonal rabbit anti-human IFN-γR2 Ab product no. 31585-1 was used at 1/1000 dilution; monoclonal mouse anti-human IFN-γR2 clone C.11 was used at 1/1000 dilution; monoclonal mouse anti-human IFN-γR2 clone MMHGR-1 was used at 1/2000 dilution. These three Abs were purchased from Preclinical Biopharmaceutics Laboratory, Rutgers University (Piscataway, NJ). Monoclonal hamster anti-human IFN-γR2 clone 2HUB159 was used at 1 μg/ml concentration; polyclonal goat anti-human IFN-γR2 was used at 0.5 μg/ml concentration. These two Abs were purchased from R&D Systems. Monoclonal mouse anti-human IFNGR2 (no. 17662-17M; U.S. Biological, Swampscott, MA) was used at 1/500 and 1/1000 dilutions. Monoclonal mouse anti-human β-actin Ab (Santa Cruz Biotechnology, Santa Cruz, CA) was used at 1/5000 dilution.

Secondary Abs

Anti-mouse HRP-conjugated Ab (Amersham Pharmacia Biotech) was used at 1/10,000 dilution. Anti-rabbit HRP-conjugated Ab was used at 1/10,000 dilution. Both Abs were from Amersham Pharmacia Biotech. Anti-hamster HRP-conjugated Ab (BD Pharmingen, San Diego, CA) was used at 1/20,000 dilution. Anti-goat HRP-conjugated Ab (Santa Cruz Biotechnology, Santa Cruz, CA) was used at 1/20,000 dilution.

Densitometry

Immunoblot films were digitized (Astra 1220U Scanner; Adobe Photoshop 6.0 software) and analyzed with the NIH Image 1.63 software.

Confocal microscopy

Images were collected on a Leica TCS-SP2 AOBS confocal microscope (Leica Microsystems, Mannheim, Germany) using a ×63 oil immersion objective numerical aperture 1.32, at different zoom factors. GFP was excited using an argon laser at 488 nm. RFP and Alexa Fluor were excited using a krypton laser at 568 mm. Differential interference contrast images

were collected simultaneous with the fluorescence images using the transmitted light detector. Z stacks of images were collected using a step increment of 0.203 μm between planes. All pictures were taken with identical settings.

Transiently transfected HEK 293 cells were incubated with the anti-GFP Alexa Fluor-conjugated Ab for 1 h at 37°C (Molecular Probes, Eugene, OR), following which the Ab-containing medium was replaced with fresh medium. Confocal microscopy was performed without cell permeabilization.

Statistical analysis

Densitometry results from the different transfection conditions were analyzed with the Microsoft Excel statistical software.

Results

Diagnosis of IFN-γR deficiency

We evaluated the IFN-γ signal transduction pathway by flow cytometric detection of phosphorylated STAT1. Phospho-STAT1 was detected in normal control PBMC after stimulation with 10 U/ml IFN-γ; patient 1 PBMC had no response even after stimulation with 10,000 U/ml (Fig. 1, IFN-γ 1000 U/ml shown). Both heterozygous parents showed phospho-STAT1 accumulation intermediate between patient 1 and the normal control (Fig. 1, mother). Native STAT1, as well as IFN-γR1, were detected at normal levels in the patient, parents, and the normal control (data not shown).

IFN-γ responsiveness was also evaluated by measurement of the ability of patient PBMC to augment LPS-induced TNF-α production in response to in vitro IFN-γ stimulation. As shown in Fig. 2, neither patient 1 PBMC obtained before bone marrow transplantation nor PBMC from patient 2 before transplant appropriately augmented LPS-induced TNF-α production in response to stimulation with IFN-γ. Under the same conditions, the heterozygous mother and father showed intermediate responses. After bone marrow transplantation patient 1 PBMC had improved their IFN-γ responsiveness to near the level of the donor mother, but not to normal levels (Fig. 2). Patient 2 and father were tested at only a single time point. Patient 2 received a bone marrow transplant early in life and therefore only one set of pretransplant PBMCs were available. We were unable to get more samples from the father to repeat the LPS and IFN-γ stimulation test.

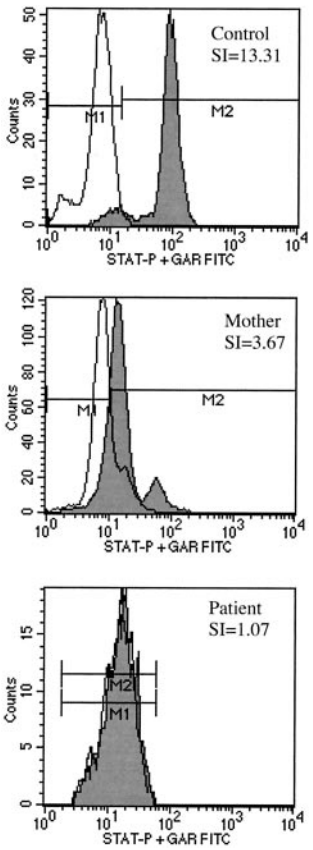

FIGURE 1. Flow cytometric intracellular detection of phospho-STAT1 is shown. PBMC from patient 1 (pre-bone marrow transplant), her mother, and a normal control were stained for phospho-STAT1 after IFN-γ stimulation (1000 U/ml for 15 min) as described (19). Phospho-STAT1 at rest (solid line) and phospho-STAT1 after IFN-γ stimulation (filled peak) are shown. Stimulation index (SI) is shown for each subject.

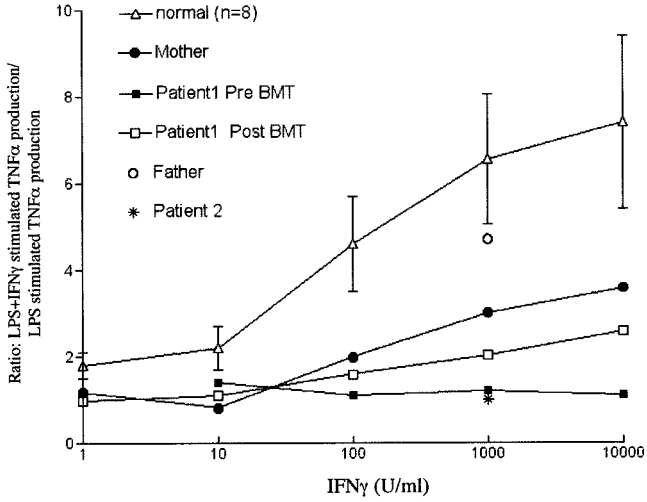

FIGURE 2. Augmentation of LPS-induced TNF-α production in response to IFN-γ stimulation. PBMC from patient 1 (pre- and post-bone marrow transplantation), patient 2, their parents, and normal controls (mean ± SE, $n = 7$) were stimulated with LPS and LPS+IFN-γ for 48 h. Cells from the father and patient 2 were studied at one dose only. Fold-TNF-α induction is the ratio of LPS and IFN-γ to LPS alone.

Diagnosis of IFN-γR2 deficiency

Genomic DNA sequencing in patients 1 and 2 showed homozygous deletion of one of two guanines at positions 791–792 in the IFNGR2 open reading frame, the region encoding the transmembrane domain. The parents were heterozygous for the same mutation. We arbitrarily designated this mutation 791delG. This missense mutation causes a frameshift and premature stop codon 8 triplets downstream. Because of the frameshift, the last eight amino acids of the wild-type transmembrane domain 243-GACF-FLVL-250 (seven hydrophobic, one hydrophilic) are predicted to be replaced by seven missense amino acids 243-EPVSSWS-249 (five hydrophilic, two hydrophobic) and a stop codon (Fig. 3). Any translated protein is predicted to include the extracellular and part of the transmembrane domains, but lack any intracellular domain.

IFNGR2 RNA was detected in patient 1, parents, and a normal control by PCR amplification of total cDNA using IFNGR2 exonic primers (Fig. 4). These PCR products were digested with *Alw*NI to probe for the restriction site introduced by mutation 791delG. As shown in Fig. 4, the wild-type control had only a single *Alw*NI-resistant band, whereas the homozygous 791delG-mutant patient 1 showed a single *Alw*NI-sensitive band, and the heterozygous parents showed two bands, one *Alw*NI-sensitive and another *Alw*NI-resistant (Fig. 4). The IFNGR2 cDNA from patient 1 was also sequenced and resulted in the predicted frameshift mutation (data not shown).

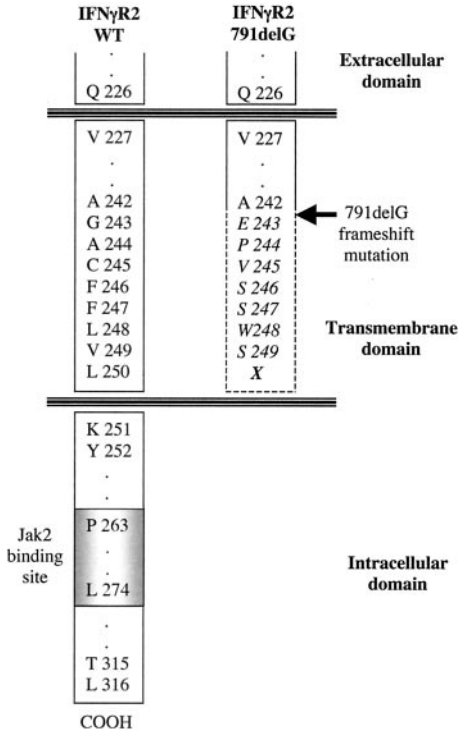

FIGURE 3. Schematic representation of IFN-γR2 wild-type and IFN-γR2 791delG-mutated alleles. IFN-γR2-numbered amino acids (boxed) and amino acid changes introduced by 791delG mutation (italic) are shown.

Immunoblotting of native IFN-γR2

Multiple Abs were used in an attempt to detect native IFN-γR2 in primary cells and cell lines. In this endeavor, we were careful to use not only normal cells as positive controls but cells from a patient previously identified as having complete recessive IFN-γR2 deficiency due to 278delAG. Abs C.11, MMHGR-2, 31585-1 (Preclinical Biopharmaceutics Laboratory), 2HUB159, and AF773 (R&D Systems), and 17662–17M (U.S. Biological) were able to detect IFN-γR2 when overexpressed as a fusion protein, but not in the native state in immunoblotting, immunoprecipitation, or flow cytometry. Therefore, we abandoned the use of commercial Abs and focused on the use of functional fusion constructs.

In vitro functional experiments

The wild-type construct SP/GFP/IFNGR2 and the mutant construct SP/GFP/791delG expressed different length GFP-IFN-γR2 fusion proteins, according to their respective IFN-γR2 MPs (Fig. 5). The wild-type construct reconstituted IFN-γ responsiveness when transiently transfected into IFN-γR2-deficient fibroblasts, as evaluated by phospho-STAT1 accumulation (19). In contrast, transfections with SP/GFP/791delG or SP/GFP/278del2 did not support IFN-γ response (Fig. 6*a*).

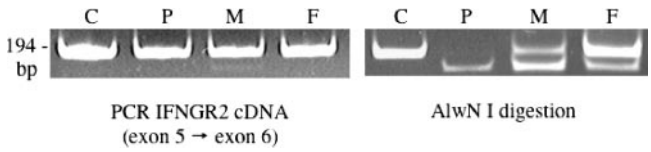

FIGURE 4. IFNGR2 cDNA/AlwN I digestion. PCR products (*left*) encompassing base 791delG IFNGR2 from control (C), patient 1 (P), mother (M), and father (F). Total cDNA was used as template. The same PCR products (3 μl) were digested with restriction enzyme *Alw*NI (*right*), which recognizes a site introduced by 791delG but not present in wild-type cDNA.

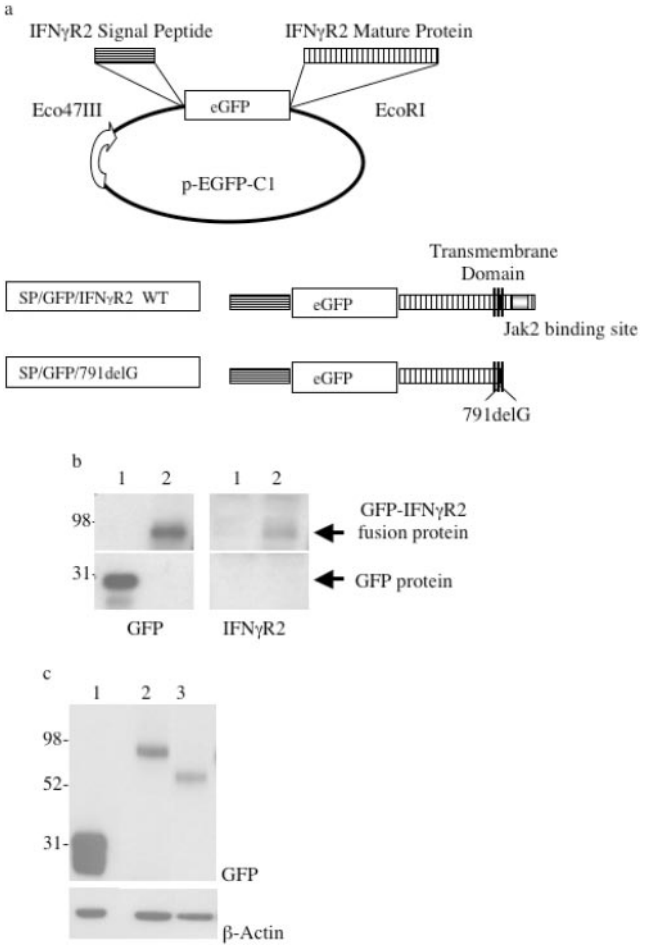

FIGURE 5. IFN-γR2 construct design and expression. *a*, IFN-γR2 expression construct design and cloning strategy including SP (▤); eGFP cassette (eGFP boxed); IFNGR2 MP coding sequence (▥); transmembrane domain (▥); Jak2 binding site (□). *b*, Immunoblot: HEK 293 cells were transiently transfected with p-eGFP-C1 and SP/GFP/IFN-γR2 clones. Immunoblots for GFP and IFN-γR2 were run in parallel. Vectors p-eGFP-C1 (1) and SP/GFP/IFN-γR2 (2) expressed GFP (*left*). Only the SP/GFP/IFN-γR2 clone expressed IFN-γR2 protein (*right*). Fusion proteins ran at the same m.w. when stained with either anti-GFP Ab or rabbit anti-human IFN-γR2 Ab no. 31585-1. *c*, Immunoblot: HEK 293 cells were transiently transfected with p-eGFP-C1 (1), SP/GFP/IFNGR2 (2), and SP/GFP/791delG (3). The different m.w. fusion proteins were evaluated with anti-GFP Ab. GFP to β-actin ratio densitometry: wild-type SP/GFP/IFNGR2, 1.0 (arbitrarily designated); SP/GFP/791delG, 0.92 (representative experiment shown). No significant differences in transfection efficiency rate or protein expression rate were detected between the wild-type SP/GFP/IFNGR2 and the SP/GFP/791delG mutant.

Cotransfections of wild-type and 791delG constructs at equal ratios (1:1) showed significant inhibition of IFN-γ-stimulated phospho-STAT1 accumulation in IFN-γR2-deficient fibroblasts when compared with cells transfected with equal amounts of the wild-type construct alone (inhibition: 48.7 ± 5%, $p < 0.001$) (Fig. 6*a*). However, no such inhibition was detected when SP/GFP/278del2 was cotransfected with SP/GFP/IFN-γR2 (Fig. 6*a*). These data indicate a dominant negative activity of 791delG over the wild-type IFN-γR2 allele when coexpressed in the context of an IFN-γR2-deficient fibroblast. When the 791delG mutant was transfected into HEK 293 cells, which contain two native IFN-γR2 alleles, we were unable to demonstrate dominant suppression of STAT1 phosphorylation. This likely reflects the compounded effects of low transfection efficiency and modest levels of suppression.

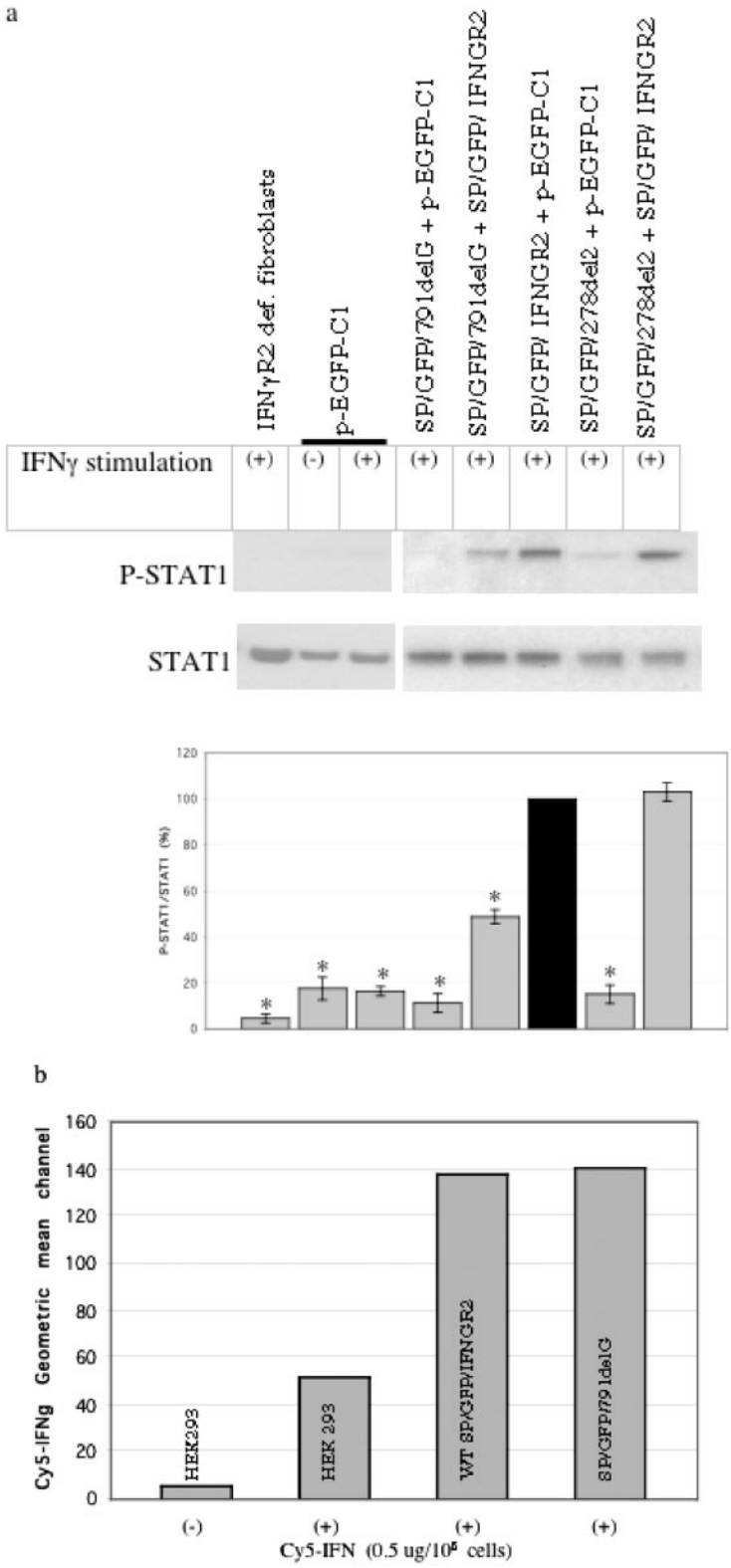

FIGURE 6. Immunoblot and binding analysis. *a*, Immunoblot of transiently transfected IFN-γR2-deficient fibroblasts. Various combinations of IFN-γR2 vectors and p-eGFP-C1 (irrelevant vector) were used to determine the functional capacity of the mutant constructs and their exertion of dominant or recessive effects. Cells were transfected with a total of 2 μg of DNA: 2 μg of a single plasmid or 1 μg of each construct in cotransfection experiments. Cells were stimulated with IFN-γ 1000 U/ml for 15 min before harvesting as indicated. Bars show the density of p-STAT1 to STAT1 ratio for each transfection condition (mean ± SE); ∗, $p < 0.001$ when compared with SP/GFP/IFNGR2 + p-eGFP-C1. *b*, Flow cytometry-based binding analysis. One million HEK 293 cells (untransfected or transfected with different constructs) were stimulated with 0.5 μg of Cy5-IFN-γ for 15 min at 4°C. After gating on the GFP-positive cells (cells successfully transfected with the GFP-tagged vectors), Cy5 geometric mean channel values were determined. Ten thousand events were acquired in a FACScan flow cytometer and analyzed using CellQuest (BD Biosciences).

We tested the hypothesis that mutant 791delG could be exerting its dominant negative effect by interfering in the IFN-γ binding to the IFN-γR complex receptor. To evaluate this possibility, we performed a flow cytometry-based binding assay in transiently transfected HEK 293 cells that naturally express native IFN-γR2. No significant differences in IFN-γ binding were detected between the wild-type and 791delG mutant transfected cells (Fig. 6*b*). To determine the specificity of 0.5× Cy5-IFN-γ binding to the IFN-γR complex in HEK 293 cells, we successfully competed away the conjugated ligand with increasing amounts of unconjugated IFN-γ (20).

Cellular distribution

Confocal microscopy of transfected HEK 293 cells showed strikingly different subcellular distributions of the fusion proteins produced by SP/GFP/IFN-γR2 and SP/GFP/791delG (Fig. 7). Cells transfected

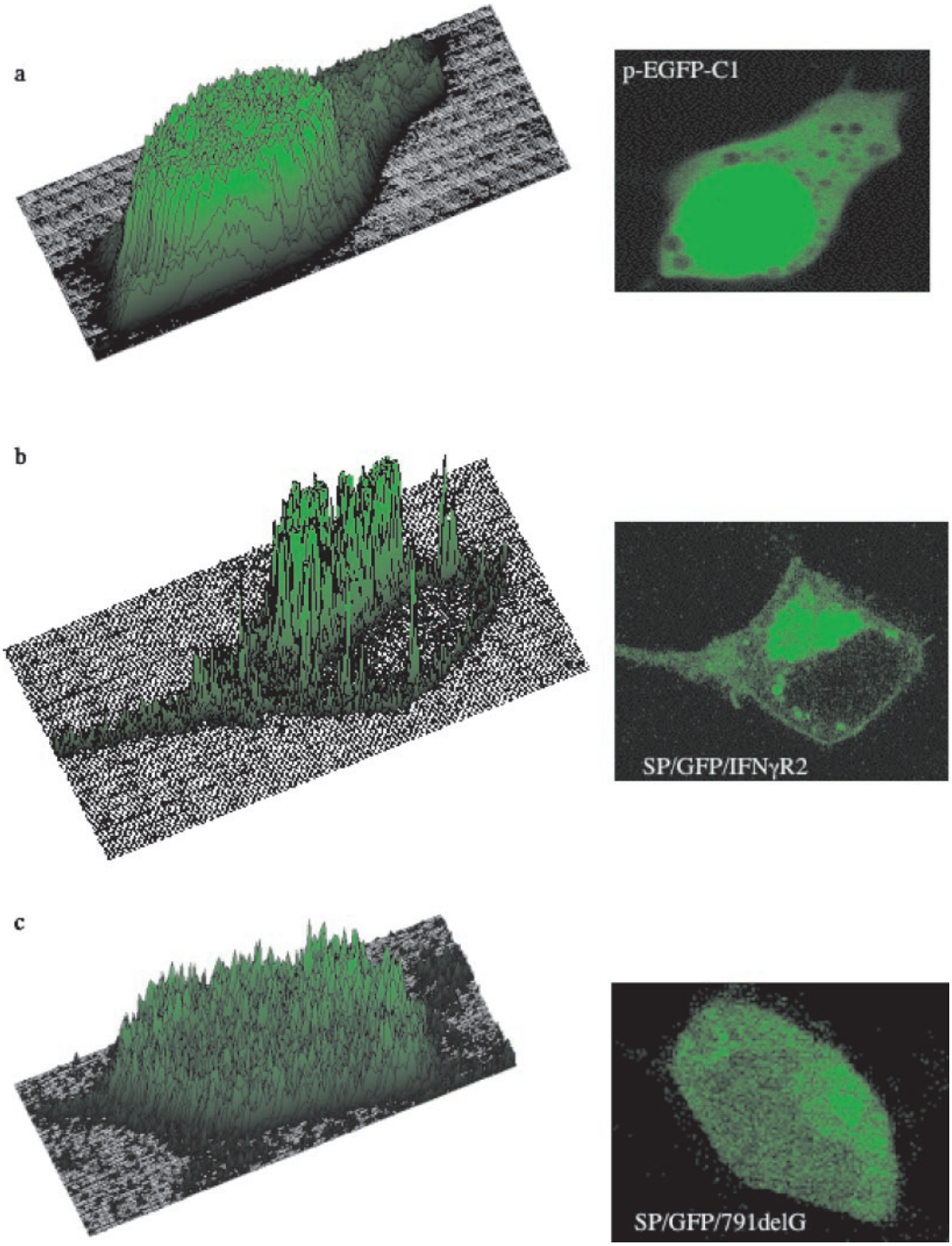

FIGURE 7. Confocal microscopy of transiently transfected HEK 293 cells. HEK 293 cells were transiently transfected with p-eGFP-C1 (*a*), SP/GFP/IFN-γR2 (*b*), or SP/GFP/791delG (*c*) for 48 h. Confocal micrographs (*right*) of representative cells. The same pictures (*left*) digitized using NIH Image 1.63 software.

with wild-type constructs showed fusion protein accumulation consistent with the native IFN-γR2 protein distribution described in several cell lines: predominantly cytoplasmic accumulation with some plasma membrane staining (1, 7, 8, 22). In contrast, the fusion protein produced by the SP/GFP/791delG mutant showed an almost uniform cytoplasmic and nuclear fine granular distribution, with striking plasma membrane exclusion (Fig. 7). Two additional experiments were performed to confirm the loss of surface expression of SP/GFP/791delG in transiently transfected HEK 293 cells. Alexa Fluor-conjugated anti-GFP Ab was tested by confocal microscopy, and an anti-GFP mAb was tested by flow cytometry analysis. Neither of these methods was able to detect surface expression of SP/GFP/791delG despite being clearly positive in wild-type transfected cells (data not shown).

When HEK 293 cells were cotransfected with equal amounts of SP/GFP/791delG and wild-type SP/RFP/IFNGR2, and despite the quantitative and qualitative differences of GFP and RFP constructs, both constructs appear to keep their respective distribution patterns (Fig. 8).

Because the cellular distribution of the IFN-γR2 791delG mutant was quite unexpected, we sought to determine whether its membrane exclusion and cytoplasmic distribution reflected pre- or

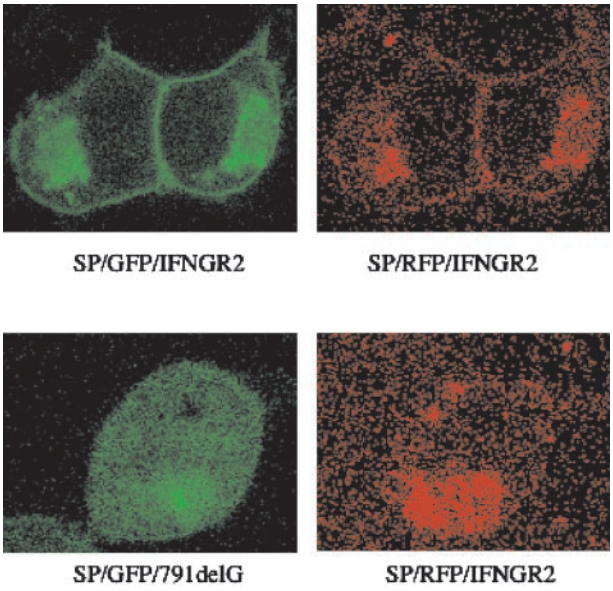

FIGURE 8. Confocal microscopy of transiently cotransfected HEK 293 cells. HEK 293 cells were transiently cotransfected with wild-type SP/GFP/IFNGR2 and wild-type SP/RFP/IFNGR2 (*top panels*) or mutant SP/GFP/791delG and wild-type SP/RFP/IFNGR2 (*bottom panels*) to assess the effects of mutant and wild-type vectors on each others' distribution. SP/GFP/IFNGR2 and SP/RFP/IFNGR2 colocalize, but SP/GFP/IFNGR2 shows a significantly stronger signal than SP/RFP/IFNGR2 (*top*). Mutant SP/GFP/791delG did not alter SP/RFP/IFNGR2 localization pattern (*bottom*). Each individual vector maintained the same distribution and accumulation pattern as shown in single vector transfections (data not shown).

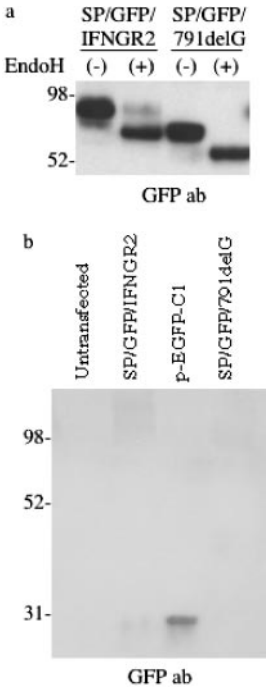

FIGURE 9. Fusion protein fate: immunoblot of EndoH digested lysates from wild-type and 791delG mutant transfected cells (*a*) and immunoblot of concentrated supernatants of untransfected or transfected HEK 293 cells (*b*). *a*, Total cell lysates (10 μg) from HEK 293 transfected cells were digested with EndoH. *b*, Supernatants of cells untransfected and transfected with SP/GFP/IFNGR2, p-eGFP-C1, and SP/GFP/791delG HEK 293 cells were collected and concentrated as described in the *Materials and Methods*.

post-Golgi processing. EndoH is a high-mannose cleaving enzyme, and *N*-glycosylated transmembrane proteins, such as IFN-γR2, become EndoH-resistant in the Golgi on their way to the plasma membrane. EndoH digestion of the fusion protein produced by SP/GFP/IFNGR2 showed both EndoH-resistant and EndoH-sensitive bands (Fig. 9*a*). In contrast, the fusion protein produced by SP/GFP/791delG yielded only a single EndoH-sensitive band (Fig. 9*a*). Therefore, some wild-type fusion protein has acquired EndoH resistance (completed Golgi processing), whereas none of the fusion protein produced by mutant SP/GFP/791delG was acquired. The plasma membrane to Golgi accumulation ratio of GFP-IFN-γR2 fusion protein in SP/GFP/IFNGR2 transfected HEK 293 cells (Fig. 7*b*) correlated with the EndoH-resistant to EndoH-sensitive bands ratios seen on Fig. 9*a* for the wild type. The diffuse cytoplasmic to Golgi accumulation ratios of the fusion protein seen in Fig. 7*c* correlated with the EndoH-sensitive lower band seen in Fig. 9*a* for 791delG. Neither SP/GFP/IFNGR2 nor SP/GFP/791delG fusion proteins were detected in the supernatants of transiently transfected HEK 293 cells (Fig. 9*b*).

Discussion

Two siblings developed severe disseminated mycobacterial infections in the setting of complete IFN-γR deficiency due to a novel homozygous mutation in the IFNGR2, 791delG. Although the parents were healthy, they showed intermediate IFN-γR activity in vitro. Interestingly, in the heterozygous parents the intermediate levels of STAT1 phosphorylation and TNF-α production in response to IFN-γ stimulation were consistent, in that the degree of reduction in STAT1 phosphorylation was similar to the reduction in TNF-α production. After successful bone marrow transplantation from the heterozygous mother, patient 1 recovered partial IFN-γR function and successfully cleared her mycobacterial infection, indicating that even the intermediate heterozygous level of IFN-γR function was adequate for both prevention (in the donor) and treatment (in the recipient) of mycobacterial infections. Because we had previously shown the absence of haploinsufficiency in complete autosomal recessive IFN-γR2 deficiency (17), we hypothesized that 791delG might exert an autosomal dominant negative effect in vitro. To further characterize this mutation, we created functional fluorescent fusion molecules.

When cotransfected with wild-type constructs, 791delG fusion proteins inhibited IFN-γ responsiveness by ~50%. Importantly, this inhibitory effect by 791delG occurs in the setting of a novel cellular distribution characterized by plasma membrane exclusion and diffuse intracellular accumulation. This distribution is quite distinct from that of the wild-type constructs, which retain a native distribution pattern. Therefore, the inhibitory activity due to 791delG occurs in the setting of a novel cellular distribution and in the absence of any detectable membrane display. This cellular distribution is likely determined by the amino acid changes in the transmembrane domain disabling Golgi processing and subsequent cell surface expression. The lack of surface expression, lack of shedding into the medium, and failure to acquire EndoH resistance indicate that this mutant's dominant effect is through a different mechanism than overaccumulation on the cell surface with competition for ligand.

Using a flow cytometry-based binding assay (21), we evaluated the effect of mutant 791delG overexpression on IFN-γ binding capacity on HEK 293 transfected cells. No differences in IFN-γ binding were detected between the wild-type and the 791delG mutant transfected cells. Therefore, interference with IFN-γ binding to the IFN-γR complex does not appear to be the mechanism involved in the 791delG dominant negative effect.

Transdominant mutants in IFNGR2 have not been previously reported. The dominant clinical phenotype and transmission patterns found in the dominant partial IFNGR1 mutants have been associated with plasma membrane overaccumulation of truncated

mutants with preserved IFN-γ binding, which are thought to disrupt the stoichiometry of the IFN-γR complex. This effect has been demonstrated in humans and mice, as well as in vitro (12, 13, 15, 23, 24). However, heterozygosity for 791delG was associated with ~50% of inhibition of the IFN-γ response both in native human cells and in transfection experiments. In native cells, this was not due to alteration of the cellular accumulation or localization pattern of IFN-γR1 (as determined by flow cytometry). In transfected cells there was no detectable effect of 791delG mutants on cotransfected wild-type IFN-γR1 or IFN-γR2. Therefore, it seems unlikely that this mutant form of IFN-γR2 is exerting its inhibitory effect on IFN-γ signaling through the previously proposed mechanism for IFN-γR1 dominant negative activity, competition for receptor binding to ligand and to authentic receptor.

The functional consequences of 791delG in either the heterozygous or homozygous states are consistent in degree between early (IFN-γ-induced STAT1 phosphorylation) and late (IFN-γ-induced TNF-α production) steps in the IFN-γ response pathway. Patient cells showed no STAT1 phosphorylation or TNF-α up-regulation after IFN-γ stimulation. In contrast, the heterozygous parents showed intermediate values of both STAT1 phosphorylation and TNF-α up-regulation. In support of these in vitro observations in primary cells, our constructs and transfections faithfully mimicked the 791delG homozygous and heterozygous states. Because the effect of these mutants is consistent between early and late responses, and our mutant construct inhibits STAT1 phosphorylation, the inhibitory mechanism by which 791delG acts is likely to be at or before STAT1 phosphorylation, with its effect maintained throughout the IFN-γ response.

The heterozygous parents, whose cells have only partial response to IFN-γ in vitro, have not developed manifestations consistent with IFN-γ receptor deficiency, despite exposures to BCG, CMV, and nontuberculous mycobacteria. In addition, bone marrow heterozygous for 791delG, in the setting of multidrug chemotherapy, was able to cure disseminated nontuberculous mycobacterial infection. Therefore, 791delG does not behave as a clinically identifiable autosomal dominant trait, at least not at this point in the parents' lives. However, mutation 791delG produced a consistent and reproducible biological effect on IFN-γ signaling in primary cells and in transfection. Interestingly, IFN-γ-induced TNF-α up-regulation in the 791delG heterozygous parents (3.85- ± 1.9-fold) was similar to that seen in patients heterozygous for IFN-γR1 818del4 dominant negative mutation (3.80- ± 0.8-fold), and intermediate to 791 homozygous (1.1- ± 0.1-fold) and normal controls (6.5- ± 1.5-fold). Patients heterozygous for IFN-γR1 818del4 often develop mycobacterial infections, especially involving the bone, which has not happened to date in the parents with heterozygous 791delG. This may reflect that IFN-γ-dependent STAT1-independent limbs of host defense may be functional in these parents providing protection above the level of the IFN-γ response alone (25–27). Regardless of the mechanisms involved, intermediate IFN-γ responsiveness due to mutation 791delG was sufficient to provide protection and to clear mycobacterial infection. A close follow up of the 791delG heterozygotes will help determine whether this mutation is clinically dominant. However, the demonstration of a mutation in IFN-γR2 that exerts a dominant negative effect in vitro without plasma surface display or impairment of wild-type IFN-γR expression suggests an as yet unrecognized component to IFN-γ signaling.

References

1. Bach, E. A., M. Aguet, and R. D. Schreiber. 1997. The IFNγ receptor: a paradigm for cytokine signaling. *Annu. Rev. Immunol. 15:563.*
2. Pernis, A., S. Gupta, K. J. Gollob, E. Garfein, R. L. Coffman, C. Schindler, and P. Rothman. 1995. Lack of interferon-γ receptor β chain and the prevention of interferon-γ signaling in Th1 cells. *Science 269:246.*
3. Bach, E. A., S. J. Szabo, A. S. Dighe, A. Ashkenazi, M. Aguet, K. M. Murphy, and R. D. Schreiber. 1995. Ligand-induced autoregulation of IFN-γ receptor β chain expression in T helper cell subsets. *Science 270:1215.*
4. Sakatsume, M., and D. S. Finbloom. 1996. Modulation of expression of the IFN-γ receptor β-chain controls responsiveness to IFN-γ in human peripheral blood T cells. *J. Immunol. 156:4160.*
5. Larkin, J., III, H. M. Johnson, and P. S. Subramaniam. 2000. Differential nuclear localization of the IFNGR-1 and IFNGR-2 subunits of the IFNγ receptor complex following activation by IFNγ. *J. Interferon Cytokine Res. 20:565.*
6. Bernabei, P., A. Allione, L. Rigamonti, M. Bosticardo, G. Losana, I. Borghi, G. Forni, and F. Novelli. 2001. Regulation of interferon-γ receptor (IFN-γR) chains: a peculiar way to rule the life and death of human lymphocytes. *Eur. Cytokine Network 12:6.*
7. Bernabei, P., E. Coccia, L. Rigamonti, M. Bosticardo, G. Losana, G. Forni, S. Pestka, C. D. Krause, A. Battistini, and F. Novelli. 2001. Interferon-γ receptor 2 expression as the deciding factor in human T, B, and myeloid cell proliferation and death. *J. Leukocyte Biol. 70:950.*
8. Rigamonti, L., S. Ariotti, G. Losana, R. Gradini, M. A. Russo, E. Jouanguy, J.-L. Casanova, G. Forni, and F. Novelli. 2000. Surface expression of the IFN-γR2 chain is regulated by intracellular trafficking in human T lymphocytes. *J. Immunol. 164:201.*
9. Newport, M. J., C. M. Huxley, S. Huston, C. M. Hawrylowicz, B. A. Oostra, R. Williamson, and M. Levin. 1996. A mutation in the interferon-γ-receptor gene and susceptibility to mycobacterial infection. *N. Engl. J. Med. 335:1941.*
10. Jouanguy, E., F. Altare, S. Lamhamedi, P. Revy, J. F. Emile, M. Newport, M. Levin, S. Blanche, E. Seboun, A. Fischer, and J.-L. Casanova. 1996. Interferon γ receptor deficiency in an infant with fatal bacille Calmette-Guérin infection. *N. Engl. J. Med. 335:1956.*
11. Holland, S. M., S. E. Dorman, A. Kwon, I. F. Pitha-Rowe, D. M. Frucht, S. M. Gerstberger, G. J. Noel, P. Vesterhus, M. R. Brown, and T. A. Fleisher. 1998. Abnormal regulation of interferon-γ, interleukin-12, and tumor necrosis factor-α in human interferon-γ receptor 1 deficiency. *J. Infect. Dis. 178:1095.*
12. Jouanguy, E., S. Lamhamedi-Cherradi, D. Lammas, S. E. Dorman, M. C. Fondaneche, S. Dupuis, R. Doffinger, F. Altare, J. Girdlestone, J.-F. Emile, et al. 1999. A human IFNGR1 small deletion hotspot associated with dominant susceptibility to mycobacterial infection. *Nat. Genet. 21:370.*
13. Villela, A., C. Picard, E. Jouanguy, S. Dupuis, S. Popko, N. Abughli, H. Meyerson, J.-L. Casanova, and R. W. Hostoffer. 2001. Recurrent *Mycobacterium avium* osteomyelitis associated with a novel dominant negative interferon γ receptor mutation. *Pediatrics 107:e47.*
14. Allende, L. M., A. Lopez-Goyanes, E. Paz-Artal, A. Corell, M.-A. Garcia-Perez, P. Varela, A. Scarlpellini, S. Negreira, E. Palenque, and A. Arnaiz-Villena. 2001. A point mutation in a domain of γ interferon receptor 1 provokes severe immunodeficiency. *Clin. Diagn. Lab. Immunol. 8:133.*
15. Waibel, K. H., D. P. Regis, G. Uzel, S. D. Rosenzweig, and S. M. Holland. 2002. Fever and leg pain in a 42-month-old. *Ann. Allergy Asthma Immunol. 89:239.*
16. Rosenzweig, S., S. E. Dorman, J. Roesler, J. Palacios, M. Zelazko, and S. M. Holland. 2002. 561del4 defines a novel deletion hotspot in the interferon γ receptor 1 chain. *Clin. Immunol. 102:25.*
17. Dorman, S. E., and S. M. Holland. 1998. Mutation in the signal-transducing chain of the interferon-γ receptor and susceptibility to mycobacterial infection. *J. Clin. Invest. 101:2364.*
18. Doffinger, R., E. Jouanguy, S. Dupuis, M. C. Fondaneche, J. L. Stephan, J. F. Emile, S. Lamhamedi-Cherradi, F. Altare, A. Pallier, G. Barcenas-Morales, et al. 2000. Partial interferon-γ receptor signaling chain deficiency in a patient with BCG and *Mycobacterium abscessus* infection. *J. Infect. Dis. 181:379.*
19. Fleisher, T. A., S. E. Dorman, J. A. Anderson, M. Vail, M. R. Brown, and S. M. Holland. 1999. Detection of intracellular phosphorylated STAT-1 by flow cytometry. *Clin. Immunol. 90:425.*
20. Rosenzweig, S. D., O. M., Schwartz, M. R. Brown, T. L. Leto, and S. M. Holland. 2004. Characterization of a dipeptide motif regulating IFNγ receptor 2 plasma membrane accumulation and IFN-γ responsiveness. *J. Immunol. 173:3991.*
21. Chianelli, M., A. Signore, R. Hicks, R. Testi, M. Negri, and P. C. L. Beverley. A simple method for the evaluation of receptor binding capacity of modified cytokines. 1993. *J. Immunol. Methods 166:177.*
22. Novelli, F., M. M. D'Elios, P. Bernabei, L. Ozman, L. Rigamonti, F. Allmerigogna, G. Forni, and G. Del Prete. 1997. Expression and role in apoptosis of the α- and β-chain of the IFN-γ receptor on human Th1 and Th2 clones. *J. Immunol. 159:206.*
23. Farrar, M. A., J. Fernandez-Luna, and R. D. Schreiber. 1991. Identification of two regions within the cytoplasmic domain of the human interferon-γ receptor required for function. *J. Biol. Chem. 266:19626.*
24. Arend, S. M., R. Janssen, J. J. Gosen, H. Waanders, T. de Boer, T. H. M. Ottenhoff, and J. T. van Dissel. 2001. Multifocal osteomyelitis caused by nontuberculous mycobacteria in patients with genetic defect of the interferon-γ receptor. *Neth. J. Med. 59:140.*
25. Ramana, C. V., N. Grammatikakis, M. Chernov, H. Nguyen, K. C. Goh, B. R. Williams, and G. R. Stark. 2000. Regulation of c-*myc* expression by IFN-γ through Stat1-dependent and -independent pathways. *EMBO J. 19:263.*
26. Ramana, C. V., M. P. Gil, Y. Han, R. M. Ransihoff, R. D. Schreiber, and G. R. Stark. 2001. Stat-1 independent regulation of gene expression in response to IFN-γ. *Proc. Natl. Acad. Sci. USA 98:6674.*
27. Gil, M. P., E. Bohn, A. K. O'Guin, C. V. Ramana, B. Levine, G. R. Stark, H. W. Virgin, and R. D. Schreiber. 2001. Biologic consequences of Stat-1 independent IFN signaling. *Proc. Natl. Acad. Sci. USA 98:6680.*